

Electrochemical Capacitance of a Nanoporous Composite of Carbon Nanotubes and Polypyrrole

Mark Hughes, George Z. Chen,* Milo S. P. Shaffer, Derek J. Fray, and Alan H. Windle

Department of Materials Science and Metallurgy, University of Cambridge, Pembroke Street, Cambridge CB2 3QZ, United Kingdom

Received August 8, 2001. Revised Manuscript Received December 21, 2001

This work reports the supercapacitive properties of electrochemically grown composite films of multiwalled carbon nanotubes (MWNT) and polypyrrole (PPy), a conducting polymer. Scanning electron microscopy, cyclic voltammetry, and electrochemical impedance spectroscopy revealed that the nanoporous three-dimensional arrangement of PPy-coated MWNTs in these films facilitated improved electron and ion transfer relative to pure PPy films. The low-frequency capacitance was measured for films of varying thickness, revealing specific capacitances per mass (C_{mass}) and geometric area (C_{area}) as high as 192 F g⁻¹ and 1.0 F cm⁻², respectively. Rates of charge and discharge about an order of magnitude faster than similarly prepared pure PPy films were also observed.

Introduction

Growing demands in digital communication, electric vehicles, and other devices that require electrical energy at high power levels in relatively short pulses have prompted considerable interest in electrochemical capacitors, also known as supercapacitors.^{1,2} The largest charge storage capabilities of supercapacitors reported to date have been observed for conducting polymers ($C_{\text{mass}} = 220 \text{ F g}^{-1}$ and $C_{\text{area}} = 600 \text{ mF cm}^{-2}$)^{3–8} and transition metal oxides ($C_{\text{mass}} = 840 \text{ F g}^{-1}$ and $C_{\text{area}} = 500 \text{ mF cm}^{-2}$)^{9–14} which store charge, in the form of ions, via a redox pseudocapacitive charge storage mechanism.^{15–17} This mechanism relies on the transfer of counterions between the electrolyte and the bulk of these materials in response to the electron-transfer

processes associated with their oxidation and reduction. Alternatively, supercapacitors made from high area carbons are attractive for their excellent rates of charge and discharge, a property stemming from their high surface area and double-layer charge storage mechanism.^{18–20} Rather than storing charge in the bulk of the capacitive material, double-layer supercapacitors store charge in an electrochemical double-layer formed at their interface with the electrolyte. While this mechanism can increase the rate of response by several orders of magnitude, it limits the total amount of charge that can be stored ($C_{\text{mass}} = 180 \text{ F g}^{-1}$ and $C_{\text{area}} = 5 \text{ mF cm}^{-2}$) relative to redox pseudocapacitive materials.^{21–25}

Recently, a variety of methods have been reported for producing composites of redox pseudocapacitive materials (polypyrrole, polyaniline, poly(*p*-phenylenevinylene), and ruthenium oxide) and double-layer capacitive materials (activated carbon black, carbon aerogels, and carbon nanotubes).^{26–36} While the capacitance of each

* To whom correspondence should be addressed.

(1) Huggins, R. A. *Philos. Trans. R. Soc. London, Ser. A* **1996**, 354, 1555.

(2) Faggioli, E.; Rena, P.; Danel, V.; Andrieu, X.; Mallant, R.; Kahlen, H. *J. Power Sources* **1999**, 84, 261.

(3) Ghosh, S.; Ingnas, O. *Adv. Mater.* **1999**, 11, 1214.

(4) Mastragostino, M.; Arbizzani, C.; Paraventi, R.; Zanelli, A. *J. Electrochem. Soc.* **2000**, 147, 407.

(5) Fusalba, F.; Elmehdi, N.; Breau, L.; Belanger, D. *Chem. Mater.* **1999**, 11, 2743.

(6) Gurunathan, K.; Murugan, A. V.; Marimuthu, R.; Mulik, U. P.; Amalnerkar, D. P. *Mater. Chem. Phys.* **1999**, 173.

(7) Fusalba, F.; Belanger, D. *J. Phys. Chem. B* **1999**, 103, 9044.

(8) Carlberg, J. C.; Ingnas, O. *J. Electrochem. Soc.* **1997**, 144, L61.

(9) Long, J. W.; Swider, K. E.; Merzbacher, C. I.; Rolison, D. R. *Langmuir* **1999**, 15, 780.

(10) Zheng, J. P.; Jow, T. R. *J. Electrochem. Soc.* **1995**, 142, L6.

(11) Cimino, A.; Carra, S. *Electrodes of Conductive Metallic Oxides-Part A*; Trasatti, S., Ed.; Elsevier: New York, 1980; p 97.

(12) Zheng, J. P.; Cygan, P. J.; Jow, T. R. *J. Electrochem. Soc.* **1995**, 142, 2669.

(13) Miousse, D.; Lasia, A. *J. New Mater. Electrochem. Syst.* **1999**, 2, 71.

(14) Jeong, Y. U.; Manthiram, A. *Electrochem. Solid State Lett.* **2000**, 3, 205.

(15) Arbizzani, C.; Mastragostino, M.; Meneghello, L. *Electrochim. Acta* **1996**, 41, 21.

(16) Barsukov, V.; Chivikov, S. *Electrochim. Acta* **1996**, 41, 1773.

(17) Ferraris, J. P.; Eissa, M. M.; Brotherton, I. D.; Loveday, D. C.; Moxey, A. A. *J. Electroanal. Chem.* **1998**, 459, 57.

(18) Sarangapani, S.; Tilak, B. V.; Chen, C. P. *J. Electrochem. Soc.* **1996**, 143, 3791.

(19) Liu, C. Y.; Bard, A. J.; Wudl, F.; Weitz, I.; Heath, J. R. *Electrochem. Solid State Lett.* **1999**, 2, 577.

(20) Ma, R. Z.; Liang, J.; Wei, B. Q.; Zhang, B.; Xu, C. L.; Wu, D. H. *Bull. Chem. Soc. Jpn.* **1999**, 72, 2563.

(21) Niu, C. M.; Sichel, E. K.; Hoch, R.; Moy, D.; Tennent, H. *Appl. Phys. Lett.* **1997**, 70, 1480.

(22) Mund, K.; Richter, G.; Weidlich, E.; Fahlstrom, U. *PACE, Process Chem. Eng.* **1986**, 9, 1225.

(23) Sawai, K.; Ohzuku, T. *J. Electrochem. Soc.* **1997**, 144, 988.

(24) Rossier, J. S.; Girault, H. H. *Phys. Chem. Chem. Phys.* **1999**, 1, 3647.

(25) An, K. H.; Kim, W. S.; Park, Y. S.; Choi, Y. C.; Lee, S. M.; Chung, D. C.; Bae, D. J.; Lim, S. C.; Lee, Y. H. *Adv. Mater.* **2001**, 13, 497.

(26) Chen, G. Z.; Shaffer, M. S. P.; Coleby, D.; Dixon, G.; Zhou, W.; Fray, D. J.; Windle, A. H. *Adv. Mater.* **2000**, 12, 522.

(27) Fan, J. H.; Wan, M. X.; Zhu, D. B.; Chang, B. H.; Pan, Z. W.; Xe, S. S. *J. Appl. Polym. Sci.* **1999**, 74, 2605.

(28) Coleman, J. N.; Curran, S.; Dalton, A. B.; Davey, A. P.; Mccarthy, B.; Blau, W.; Barklie, R. C. *Phys. Rev. B* **1998**, 58, R7492.

(29) Curran, S. A.; Ajayan, P. M.; Blau, W. J.; Carroll, D. L.; Coleman, J. N.; Dalton, A. B.; Davey, A. P.; Drury, A.; Mccarthy, B.; Maier, S.; Strevens, A. *Adv. Mater.* **1998**, 10, 1091.

carbon-ruthenium oxide composite was lower than that reported for pure ruthenium oxide, the capacitive properties of most of the carbon-conducting polymer composites are, as yet, unknown. The limited capacitive data previously reported for high-area carbon-conducting polymer composites is restricted to composites of MWNTs and PPy or polyaniline grown by electrochemically polymerizing the conducting polymer onto a MWNT preform or by in situ chemical polymerization of the conducting polymer onto MWNTs in a suspension which is subsequently dried to a powder and pressed ($C_{\text{mass}} = 170 \text{ F g}^{-1}$ and $C_{\text{area}} = 241 \text{ mF cm}^{-2}$).^{37–39} While these particular composite systems indicate that the high surface area and conductivity of MWNTs augment the redox properties of conducting polymers, their structure and capacitance are inherently limited by their synthesis routes. Electrochemical growth techniques employing MWNT preforms are limited by the amount of polymer that can be deposited without blocking electrolyte channels, and chemical polymerization techniques can suffer from aggregation of the polymer deposited on the MWNTs. The electrochemical method used to grow the carbon nanotube-conducting polymer composites described in this report circumvents these problems via the simultaneous deposition of MWNTs and PPy during film growth in a single step.

Experimental Section

Composite films were electrolytically deposited onto a graphite working electrode in a three-electrode, single compartment electrochemical cell.²⁶ The aqueous polymerization electrolyte generally consisted of 0.5 M pyrrole monomer and 0.4 wt % of suspended oxidized MWNTs having an outer diameter of about 10 nm and a length between 0.2 and 2.5 μm .⁴⁰ Oxidation of the curved catalytically grown MWNTs (supplied by Hyperion) was achieved via a previously described acid treatment process which attaches functional groups such as hydroxyl, carbonyl, and carboxylic groups to the MWNT surface, facilitating their suspension in polar solvents such as distilled water.⁴¹ After the electrolyte was deaerated using argon, anodic polymerization of the pyrrole monomer was achieved at the working electrode using a constant current of 3.0 mA cm^{-2} or a constant potential of 0.7 V measured against a saturated calomel reference electrode (SCE). The negatively charged MWNTs acted both as a supporting electrolyte during polymerization and as a dopant in the PPy deposited on the working electrode.²⁶ Once formed, the films were analyzed using cyclic voltammetry (CV), on a model 273A EG&G Princeton Applied Research potentiostat, and electrochemical

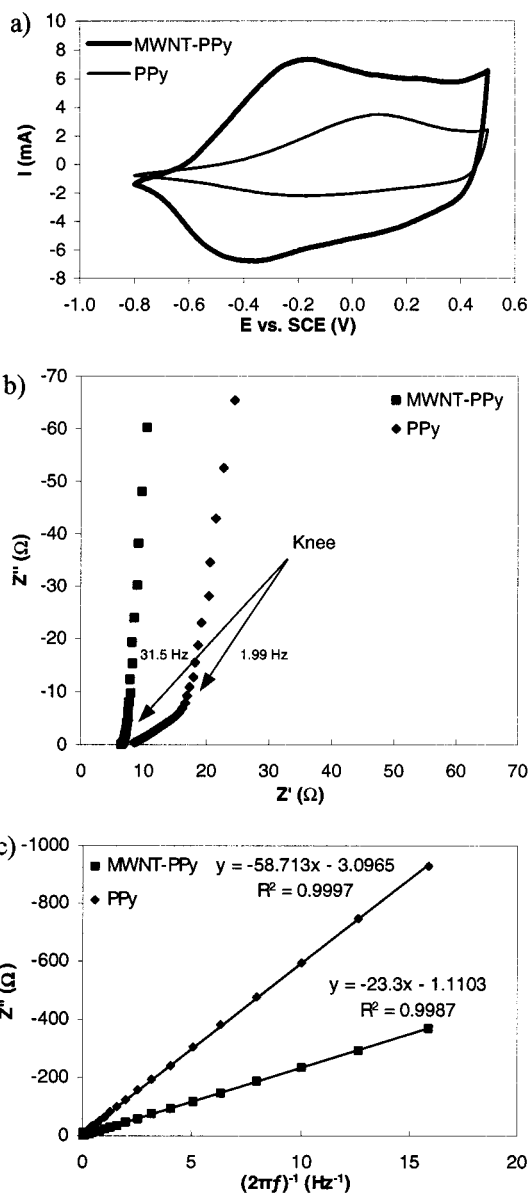


Figure 1. Comparison of MWNT–PPy composite films and pure PPy films prepared using similar conditions: (a) cyclic voltammograms (film-formation charge, 1.8 C cm^{-2} ; scan rate, 50 mV s^{-1} ; electrolyte, 0.5 M KCl); (b) complex plane impedance plots (film-formation charge, 1.0 C cm^{-2} ; bias potential, 0.4 V vs SCE; electrolyte, 0.5 M KCl); (c) relationship between the imaginary component of impedance and the inverse of frequency (film-formation charge, 1.0 C cm^{-2} ; bias potential, 0.4 V vs SCE; electrolyte, 0.5 M KCl).

impedance spectroscopy (EIS), on a Solartron 1260 impedance/gain-phase analyzer coupled with a Solartron 1287 electrochemical interface. Testing was carried out at potentials between -0.8 and 0.5 V vs SCE in a three-electrode, single compartment electrochemical cell using a deaerated 0.5 M KCl aqueous electrolyte. To provide a basis for comparison, these tests were also performed on pure PPy films made using the same setup and conditions, with the MWNTs being replaced by 0.5 M KCl in the aqueous polymerization electrolyte.

Results and Discussion

Figure 1 compares the CV and EIS results of a MWNT–PPy composite film with a similarly prepared pure PPy film. The cyclic voltammograms (Figure 1a) indicate several important differences between the two

(30) Yoshino, K.; Kajii, H.; Araki, H.; Sonoda, T.; Take, H.; Lee, S. *Fullerene Sci. Technol.* **1999**, *7*, 695.

(31) Ago, H.; Petritsch, K.; Shaffer, M. S. P.; Windle, A. H.; Friend, R. H. *Adv. Mater.* **1999**, *11*, 1281.

(32) Gao, M.; Huang, S.; Dai, L.; Wallace, G.; Gao, R.; Wang, Z. *Angew. Chem., Int. Ed.* **2000**, *39*, 3664.

(33) Miller, J. M.; Dunn, B. *Langmuir* **1999**, *15*, 799.

(34) Zheng, J. P. *Electrochem. Solid State Lett.* **1999**, *2*, 359.

(35) Lin, C.; Ritter, J. A.; Popov, B. N. *J. Electrochem. Soc.* **1999**, *146*, 3155.

(36) Ma, R.; Wei, B.; Xu, C.; Liang, J.; Wu, D. *Bull. Chem. Soc. Jpn.* **2000**, *73*, 1813.

(37) Frackowiak, E.; Jurewicz, K.; Delpeux, S.; Beguin, F. *J. Power Sources* **2001**, *97–8*, 822.

(38) Jurewicz, K.; Delpeux, S.; Bertagna, V.; Beguin, F.; Frackowiak, E. *Chem. Phys. Lett.* **2001**, *347*, 36.

(39) Downs, C.; Nugent, J.; Ajayan, P. M.; Duquette, D. J.; Sathnam, S. V. *Adv. Mater.* **1999**, *11*, 1028.

(40) Kinloch, I. Carbon Nanotubes: Production and Concentrated Dispersions. Ph.D. Thesis, University of Cambridge, Cambridge, UK, 2001; Chapter 7.

(41) Shaffer, M. S. P.; Fan, X.; Windle, A. H. *Carbon* **1998**, *36*, 1603.

films. The first of these is that the peak potentials of the composite film are about 200 mV more negative than those of the pure PPy film, confirming the anionic dopant role of the MWNTs.²⁶ The second point is that the output current of the composite film is about twice that of the pure polymer. Since capacitance can be estimated from the output current divided by the scan rate, this implies that the capacitance of the composite films is about double that of the pure polymer.^{19,39} A final point worth noting is that the difference between the output current of the composite and the pure polymer is particularly large for low oxidation potentials at which both films are in their lower conductivity reduced state, indicating a conductive contribution from the MWNTs in the composite film.²⁶

The small sine-wave amplitude (10 mV) and broad frequency range (5×10^5 Hz to 0.01 Hz) used for EIS analysis makes it possible to separate and study electrochemical processes having different time constants, such as electrical conduction, ion transfer, and capacitance, while displacing the system only slightly from its equilibrium state.^{42,43} Figure 1b shows the complex plane impedance plots produced from EIS analysis of the fully oxidized composite and pure PPy films (bias potential of 0.4 V). The intercepts of the composite and pure PPy plots with the real impedance (Z') axis, 6.4 and 8.5 Ω , respectively, indicate that the composite film was 2.1 Ω less resistive than the pure PPy film. This estimation is based on the reasonable assumption that the resistances of the electrical leads and the 0.5 M KCl electrolyte were the same in both cases, since the intercept actually reports the uncompensated electrical resistance of the capacitive film, electrolyte, and the electrical leads combined.⁴⁴ While this result is in agreement with a conductive contribution from the MWNTs, it should be noted that the reduced resistance of the composite film may in part be due to the increased surface area of the porous composite structure.

The impedance plot shown in Figure 1b can be divided into the high-frequency component (inclined at 45°) and the low-frequency component (near vertical) of the plot. The projected length of the high-frequency Warburg-type line on the real axis (Z') characterizes the slow ion migration process in the solution pores and is equal to one-third the film's ionic resistance.⁴² The composite and pure PPy films shown in Figure 1b had ionic resistances of 0.7 and 24.3 Ω , respectively, indicating a lower barrier to ionic transport in the composite film.⁴³ The superior ionic transfer of the composite films is even more exaggerated at bias potentials lower than 0.4 V and is in addition to the improved electrical conductivity of the composite films described above.

The low-frequency capacitance (C_{lf}) of the composite films was determined from the slope of a plot of the imaginary component of impedance (Z'') at low frequency vs the inverse of frequency (f) (Figure 1c) using the equation $C_{lf} = (2\pi f Z'')^{-1}$.⁵ Specific capacitances as high as 192 F g⁻¹ and 1.0 F cm⁻² were observed for the

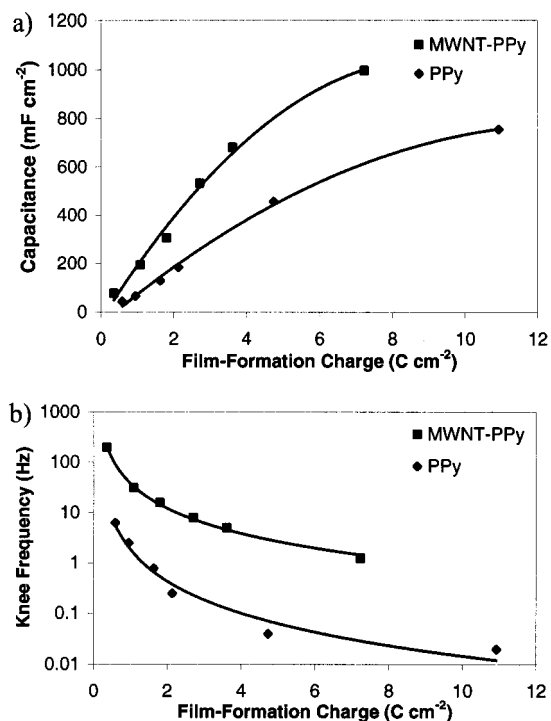


Figure 2. Relationship between film-formation charge and: (a) low-frequency capacitance and (b) knee frequency for MWNT-PPy films and similarly prepared pure PPy films.

MWNT-PPy composite films tested. While the capacitance per gram of composite film is quite high, it is the capacitance per area of deposition surface that draws the most interest. This value is significantly larger than that reported for supercapacitors based on conducting polymers, carbon nanotubes, or other carbon nanotube-conducting polymer composites.^{4,25,37-39} Figure 2a shows how the low-frequency capacitance of the composite films and similarly prepared pure PPy films increased with the film-formation charge. The film-formation charge is a measure of the total charge used during polymerization; hence, it indicates the amount of film grown providing there are no other reactions occurring at the working electrode. While the thickness of the composite and pure PPy films was found to increase approximately linearly with film-formation charge as expected⁴⁵ with slopes of 3.5×10^{-4} and 1.8×10^{-4} cm³ C⁻¹, respectively, their capacitance deviated from its initially linear relationship for large film-formation charges (Figure 2a). This deviation is attributed to limited electrolyte access at the lower levels of thick films. As a result, ion diffusion is not able to reach all the available PPy within the time frame of the capacitive measurements, thereby restricting the amount of material that can contribute to the measured capacitance, causing it to approach an upper limit with increasing film-formation charge.

The linear regions of the capacitance vs film-formation charge plots (Figure 2a) show that for a given charge, the composite film had a capacitance that was about double that of pure PPy, supporting the capacitive results obtained from the cyclic voltammograms. The slope (C/Q) of these linear regions gives an indication as to the proportion of film that contributes to the

(42) Albery, W. J.; Chen, Z.; Horrocks, B. R.; Mount, A. R.; Wilson, P. J.; Bloor, D.; Monkman, A. T.; Elliot, C. M. *Faraday Discuss. Chem. Soc.* **1989**, *88*, 247.

(43) Guerrero, D. J.; Ren, X.; Ferraris, J. P. *Chem. Mater.* **1994**, *6*, 1437.

(44) Wen, C. J.; Ho, C.; Boukamp, B. A.; Raistrick, I. D.; Weppner, W.; Huggins, R. A. *Int. Met. Rev.* **1981**, *5*, 253.

(45) Smela, E. *J. Micromech. Microeng.* **1999**, *9*, 1.

capacitive performance. The superior slope of the composite films implies that more of the PPy in the film is able to access ionic charge from solution and hence contribute to the measured capacitance. The larger limiting value of capacitance apparent for the composite films indicates that their improved performance for a given film-formation charge is not simply a result of an increase in polymerization efficiency, which would result in the deposition of more polymer for a given film-formation charge, relative to the pure PPy films. In fact, the polymerization efficiency of the composite films was found to be within a few percent of the pure PPy films making the film-formation charge a fair means of comparison.

The point that divides the high-frequency component of the complex plane impedance plot from the low-frequency component is referred to as the knee frequency²¹ (Figure 1b). The knee frequency indicates the maximum frequency at which predominantly capacitive behavior can be maintained and was more than an order of magnitude higher for MWNT-PPy composite films than pure PPy films (Figure 2b). For low film-formation charges, the knee frequency of the composite supercapacitors was as high as 200 Hz; however, as the film-formation charge was increased, the knee frequency decreased rapidly as shown in Figure 2b. This performance limitation is a common phenomenon for devices based on conducting polymers and is simply related to the reduction in electrolyte access and increase in diffusion distance with film thickness.⁴⁶

The structure of the MWNT-PPy composite films was examined using a JEOL JSM6340F field emission gun scanning electron microscope (FEGSEM). PPy was found to coat each individual MWNT and bind the coated tubes together in a nanoporous three-dimensional network (Figure 3). The thickness of the PPy coating on each tube was observed to reach as much as 250 nm depending on the polymerization conditions employed, though values much lower than this were used to obtain the results described in this report. Examination of the relative thermal degradation rates of pure PPy films, pure MWNT sheets, and MWNT-PPy composite films in air using a Perkin-Elmer Series 7 thermogravimetric analyzer ($10\text{ }^{\circ}\text{C min}^{-1}$) indicates that the polymerization conditions described in this report produced composites that were approximately 60 wt % MWNTs. It is also interesting to note that the coated MWNTs tended to preferentially align parallel to the plane of the film while maintaining random orientation within the plane, similar to the structures observed in solvent-cast MWNT films.⁴⁷ The structure of the composite film contributes to its improved ionic conductivity, capacitance, and rate of response in three ways. The first is by providing a large surface area of PPy in a porous morphology that allows excellent electrolyte access in three dimensions. Second, since the PPy is coated on each MWNT as a thin layer, the ion intercalation distance is reduced to a matter of nanometers. Finally, the conductivity of the MWNTs dispersed

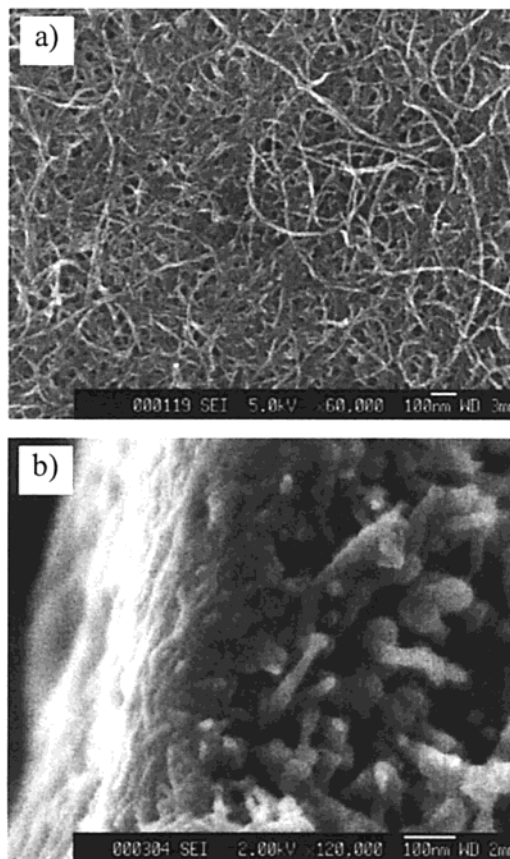


Figure 3. FEGSEM images showing the porous network of PPy-coated MWNTs in the composite films: (a) the film surface and (b) the fractured film cross-section.

throughout the structure increases the electrical conductivity of the composite film over the entire PPy redox cycle.

Conclusions

In summary, we have studied the structure and capacitive properties of composite films made from catalytically grown MWNTs and PPy. These composites were produced via an electrochemical route in which the MWNTs and PPy were deposited simultaneously. FEGSEM analysis indicated that it was possible to produce porous interconnected networks of PPy-coated MWNTs through the entire thickness of the film. CV and EIS analyses demonstrated the excellent charge storage and transfer capabilities of these films, a result that is attributed to the high surface area, conductivity, and electrolyte accessibility of the nanoporous structure. These results suggest that nanoporous composites of MWNTs and conducting polymers hold great promise for energy storage devices such as supercapacitors and secondary batteries.

Note Added after ASAP Posting

This article was released ASAP on 2/21/2002 with a minor error in the Results and Discussion section. The correct version was posted on 3/4/2002.

CM010744R

(46) Dellasanta, A.; Derossi, D.; Mazzoldi, A. *Synth. Met.* **1997**, *90*, 93.

(47) Shaffer, M. S.; Windle, A. H. *Adv. Mater.* **1999**, *11*, 937.